TECHNICAL NOTES

NATIONAL ADVISORY COMMITTEE FOR AERONAUTICS

No. 500

THE TORSIONAL STIFFNESS OF THIN DURALUMIN SHELLS SUBJECTED TO LARGE TORQUES

By Paul Kuhn
Langley Memorial Aeronautical Laboratory

Washington
July 1934

NATIONAL ADVISORY COMMITTEE FOR AERONAUTICS

TECHNICAL NOTE NO. 500.

THE TORSIONAL STIFFNESS OF THIN DURALUMIN SHELLS SUBJECTED TO LARGE TORQUES

By Paul Kuhn

SUMMARY

This report gives a simple method of estimating the torsional stiffness of thin shells, such as box beams or stressed-skin wings under large torque loads. A general efficiency chart for shells in torsion is established, based on the assumption that the efficiency of the web sheet in resisting deformation decreases linearly with the average stress. The chart is used to calculate the torsional deflections of eight box beams, a test wing panel, and a complete wing; the results of the calculations are shown in comparison with the test results. The agreement is probably as good as might be expected considering the empirical nature of the method and the well-known dispersion between results of tests on thin sheet-metal structures.

INTRODUCTION

A knowledge of the torsional stiffness of box beams and stressed-skin wings under large torsional moments is necessary for calculating the interaction between spars (reference 1). Thin shells of this nature buckle under small loads and the cover plates work no longer in shear, but in diagonal tension. This transition decreases the torsional stiffness considerably, but it is not sufficient to explain the large deformations that tests show, particularly under large loads. The experimental load-deformation diagrams are curves rather than straight lines, indicating that the torsional stiffness decreases continuously as the load increases. A method of correcting the theoretical-stiffness constants was therefore developed based on the assumption that the efficiency of the sheet metal in resisting deformation decreases linearly with the average stress in the sheet, the rate of decrease depending on the aspect ratio of the individual sheets.

CALCULATION OF THE TORSIONAL STIFFNESS OF SHELLS

When concentrated torques T act on the ends of a tube (fig. 1) of length L the resulting angle of twist is

$$\theta = \frac{TL}{GJ} \tag{1}$$

where G is the modulus of shear and

J is the torsion constant of the section.

For a thin-walled tube the torsion constant is

$$J = \frac{4A^2}{\int \frac{ds}{t}} \tag{2}$$

where A is the area bounded by the median line of the cross section, ds is a differential element of the perimeter and t is the thickness of this element. The shearing stress at any point is

$$f_s = \frac{T}{2At} \tag{3}$$

Formulas (2) and (3) are derived under the assumptions that the wall thicknesses are small and that the cross sections do not change their shape. Both formulas have been verified experimentally by various investigators and have been found to check the experimental values within very close limits for round, rectangular, and streamline tubing of the thickness-diameter ratios usual in aircraft construction.

Box spars and stressed-skin wings are also thin-walled tubes, but the wall thicknesses are very much smaller in relation to the dimensions of the cross section than in the case of tubing. When such a thin shell is subjected to torsion, the sides will buckle at a very small load and will be transformed into diagonal-tension field beams.

For the present purpose it is convenient to calculate the deflections occurring after the diagonal-tension field has formed by using the formulas for shear deflection. Consider a square sheet with a side length of unity and a thickness t, subjected to a shearing force S. If the sheet did not buckle, the shear deflection would be

$$y = \frac{S}{Gt} \qquad (4)$$

where G is the modulus of shear. If the same sheet were a panel of a Wagner beam, i.e., if it did buckle, the deflection would be

$$y = \frac{4S}{Et} \qquad (5)$$

E being the modulus of elasticity. When (4) and (5) are compared it will be seen that (4) can be used to calculate the deflection of a Wagner beam panel provided that the actual thickness t is replaced by an effective thickness

$$t_e = \frac{t}{4}\frac{E}{G} \qquad (6)$$

or, for duralumin $t_e = 5/8\ t$.

Formula (5) is based on the elementary theory of the Wagner beam presuming rigid flanges. In the particular type of structures under consideration, however, the flanges of the beams are very flexible. In some cases the flanges consist of angles of a lesser thickness than the web itself. For beams with such flexible flanges, the applicability of the theory is very doubtful. It is only known that the stress distribution in the web loses uniformity more and more while the load increases, the stress concentrating along the folds as indicated in figure 2. The effect of this change in stress distribution on the shear deflection can be indicated by writing

$$y = \frac{S}{Gt_e\eta} \qquad (7)$$

where η is an efficiency factor depending on the average stress and on the flexibility of the flanges. Since η

decreases with increasing stress, the torsional stiffness of a shell is not a constant, but decreases with increasing torque, resulting in a curved load-deformation diagram.

A convenient means of establishing empirical relations for η was afforded by the test results given in reference 2, which describes a series of tests on box beams of similar construction. The beams consisted of smooth sheets, 0.010 to 0.041 inch thick, riveted to 4-inch channels, 0.015 to 0.049 inch thick. (See figs. 5 to 12.) The bulkheads were made of sheet 0.037 to 0.049 inch thick.

It was found that η could be assumed to decrease linearly with increase of stress from unity at zero stress (fig. 3). The average shearing stress f_s calculated by formula (3) was used as an index for convenience, although this stress does not actually exist as a shearing stress after the diagonal-tension field has formed. The rate of change of efficiency with stress was found to be only a function of the spacing of the uprights supporting the flanges of the Wagner beams or, in other words, of the aspect ratio d/h of the component plates (fig. 2). This fact was somewhat surprising, because one would naturally expect the cross section of the flanges to have some influence. For the very flexible flanges, however, which are a characteristic of the beams investigated, the evidence appears to indicate that this influence is of a minor nature. Undoubtedly, flanges consisting of heavy angles, would have some such influence. The beam of figure 12 has corner reinforcements, but as the test was not carried to failure, no conclusions could be based on it.

The procedure of calculating the torsional stiffness for a given beam or shell under any given torque will therefore be as follows:

(1) Calculate the critical buckling stresses in shear for the component sheets. The edges of the sheets should be assumed to be simply supported, because the beneficial effect of the existing elastic restraint is probably more than canceled by the detrimental effect of initial buckles. The critical stress calculated is probably not conservative but is, in general, sufficiently accurate for the present purpose. Figure 4 gives a graph for calculating the buckling stresses of duralumin sheets based on values given in reference 3.

(2) Calculate f_s for each sheet by formula (3). If this stress is higher than the critical buckling stress found in step (1), use the efficiency chart (fig. 3) to find η.

(3) Calculate the torsion constant J by formula (2), substituting for the thickness the actual value t if the sheet has not buckled, or the value $t_e \times \eta = 5/8\ t\eta$ if the sheet has buckled.

In structurally complex shells, e.g., wings with several spars and longitudinal stringers, it may be difficult to decide the proper value of h to use. If longitudinal seams exist between spars in the skin, as on the panel shown in figure 13, the distance between seams should be used. In any complex, built-up shell, values of d/h less than 0.8 should be used with caution and substantiated by tests if necessary.

If it is desired to construct a load-deformation diagram, the load is divided into a number of convenient intervals, say 2,000 in.-lb. The stiffness is then calculated for the middle of each interval (1,000 in.-lb., 3,000 in.-lb., etc.) and the increment in angle of twist due to each increment of torque is calculated. The increments of twist are plotted against torque; the resultant broken line gives a series of tangents to the desired curve.

COMPARISONS BETWEEN CALCULATED AND EXPERIMENTAL DEFORMATION DIAGRAMS

Figures 5 to 12 show the calculated deflection curves and the experimental points for the beams of reference 2. The construction of all the beams is very similar. The essential dimensions are given on each figure.

The beams of figures 5, 6, and 7 are identical with the exception of bulkhead spacing. The beam of figure 9 is the only one of the series that shows considerably more deflection than predicted. No explanation could be found for this behavior. Comparative weight estimates indicate, however, that some sheets of this beam may have had less than nominal thickness. It must be remembered that the

commercial tolerance for thickness variation is 0.0015 inch or 7 percent of the top and bottom cover.

The beam of figure 10 has a cambered top cover. The buckling stress for this curved sheet was assumed to be the same as if the sheet were part of a cylinder and was calculated by the method given in reference 4.

The results on the wing panel (fig. 13) were taken from reference 5. The sheets are supported by ribs and stringers so that they are divided into nearly square component panels. The effect of the curvature on the critical buckling stress was neglected; i.e., it was assumed that the leading edge buckled at the same time as the flat part of the covering; so that $t_e = 5/8\ t$ over the whole surface. This assumption is contrary to the experimental evidence; tests always show that the sharply curved nose covering does not buckle until large loads are applied; in fact, buckling of the leading edge is usually the cause of ultimate failure of the wing shell in torsion. (See fig. 14.) However, the part of the nose that does not buckle is a small part of the whole cover. Furthermore, the cover does buckle a short distance behind the nose, where the curvature is still very large; the buckles occurring at this location tend to pull the sheet down to chord lines subtending the actual curve of the profile, thus reducing the area included by the profile forward of the front spar. This reduction of included area reduces the stiffness (formula (2)); therefore the assumption of all the covering buckling tends to give an average. The fact that the actual stiffness was larger than the calculated value is partly due to the fact that the web of the front spar was neglected in the calculation of the torsional stiffness. Inner walls, such as this spar, usually contribute less than 5 percent to the torsional stiffness of a shell but in this case the more exact formula, which includes the effect of the front spar, gave a torsional stiffness 7 percent higher than that calculated by the simple formula (2).

Figure 14 shows the calculated and the experimental twist at 5 stations of an all-metal wing (reference 6). No data were available on the spar system except photographs, which showed a multispar system similar to the Junkers type (transposed flanges) with apparently very light web members. Calculations given in reference 1 show that for 2-spar, stressed-skin wings the influence

of the spars on the torsional stiffness is negligible; the same thing is probably true for this multispar wing. The value $d/h = 1$ was used, because it is representative of the major part of the cover.

Failure occurred between stations 4 and 5 by buckling and rupture of the leading edge. The result was the large deformation recorded at station 5 for the last two load increments.

Omitting curve 2 of figure 14, because there was obviously some disturbance of the apparatus before the last three readings were taken, and also curve 5 of the same figure because failure occurred here, the average ratio of calculated to observed deflection for the last points of all test curves given is 0.92.

CONCLUSION

The method given for estimating the torsional stiffness of a thin shell under large torques cannot lay claim to great accuracy. It is empirical in nature and based on not very extensive evidence. Additional experimental or theoretical research may replace the straight lines of the efficiency chart by curves, change the spacing of the curves, and introduce the stiffnesses of the flanges and of the bulkhead as factors. Until such additional work is done, the chart may serve as a guide.

Langley Memorial Aeronautical Laboratory,
National Advisory Committee for Aeronautics,
Langley Field, Va., June 11, 1934.

REFERENCES

1. Kuhn, Paul: Analysis of 2-Spar Wings with Special Reference to Torsion and Load Transference. T. R. (to be published later). N.A.C.A.

2. Greene, C. F., and Younger, J. E.: Report on Metal Wing Construction. Part I - Experimental Studies and Discussion. Air Corps Technical Report, Serial No. 3361, Materiel Division, Army Air Corps, 1929.
Carpenter, S. R.: Report on Metal Wing Construction. Part III - Compilation of Test Data. Air Corps Technical Report, Serial No. 3333, Materiel Division, Army Air Corps, 1930.

3. Timoshenko, S.: Strength of Materials. D. Van Nostrand Company, 1930.

4. Donnell, L. H.: Stability of Thin-Walled Tubes Under Torsion. T. R. No. 479, N.A.C.A., 1933.

5. Hertel, Heinrich: Die Verdrehsteifigkeit und Verdrehfestigkeit von Flugzeugbauteilen. D.V.L. Yearbook, 1931, pp. 165-220.

6. Hickerson, R. L.: Static Test of Cairns Cantilever Monoplane Wing. Serial No. P.T.L. 35, Bureau of Aeronautics, Navy Dept., 1931.

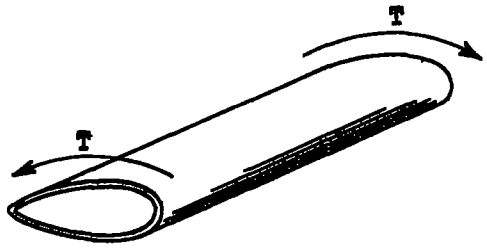

Figure 1.

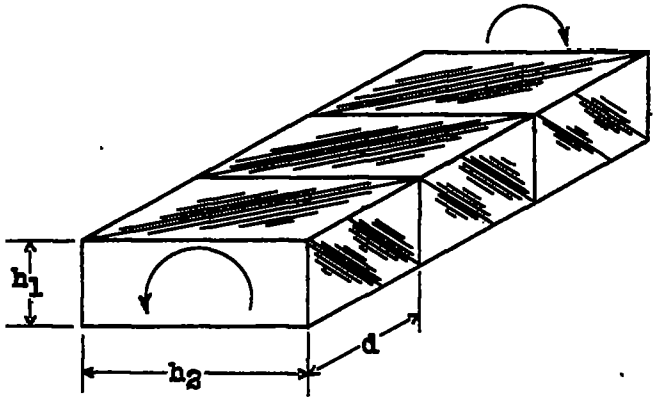

Figure 2.

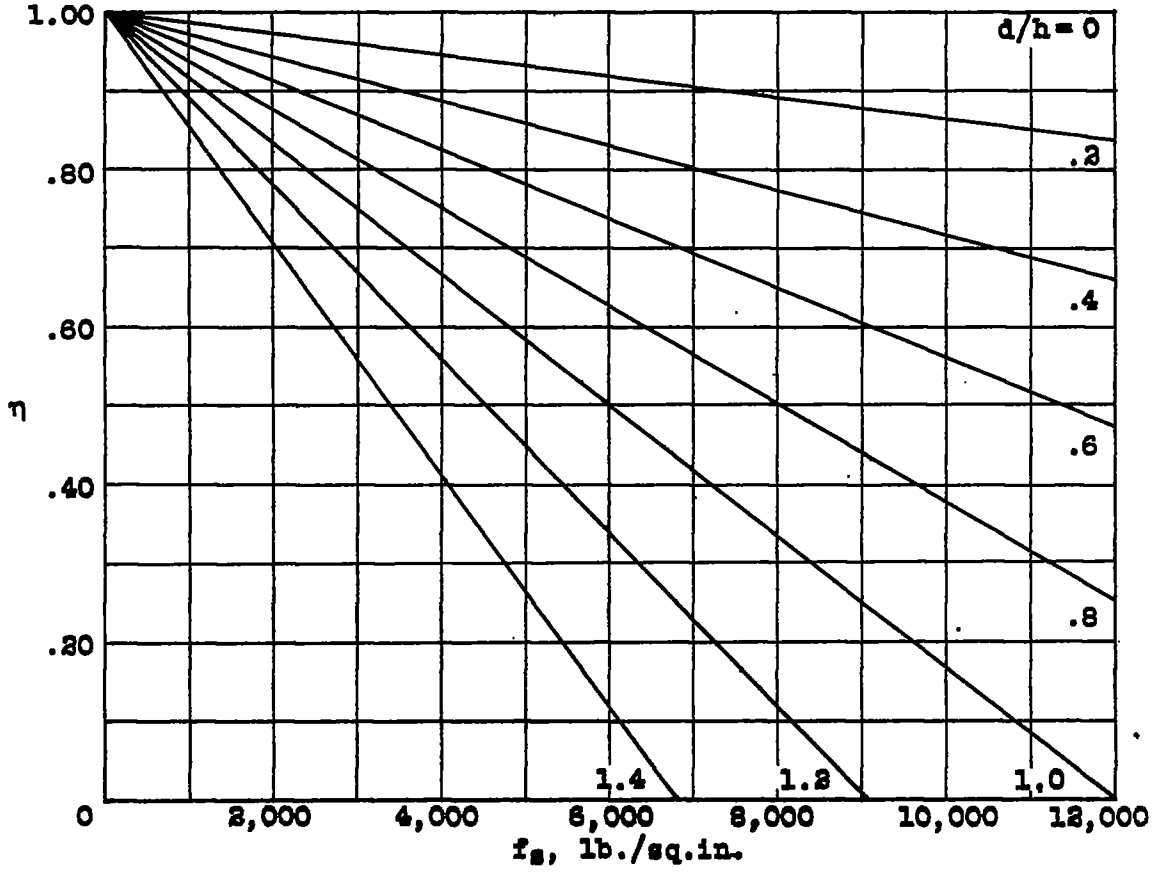

Figure 3.- Efficiency chart for thin shells in torsion.

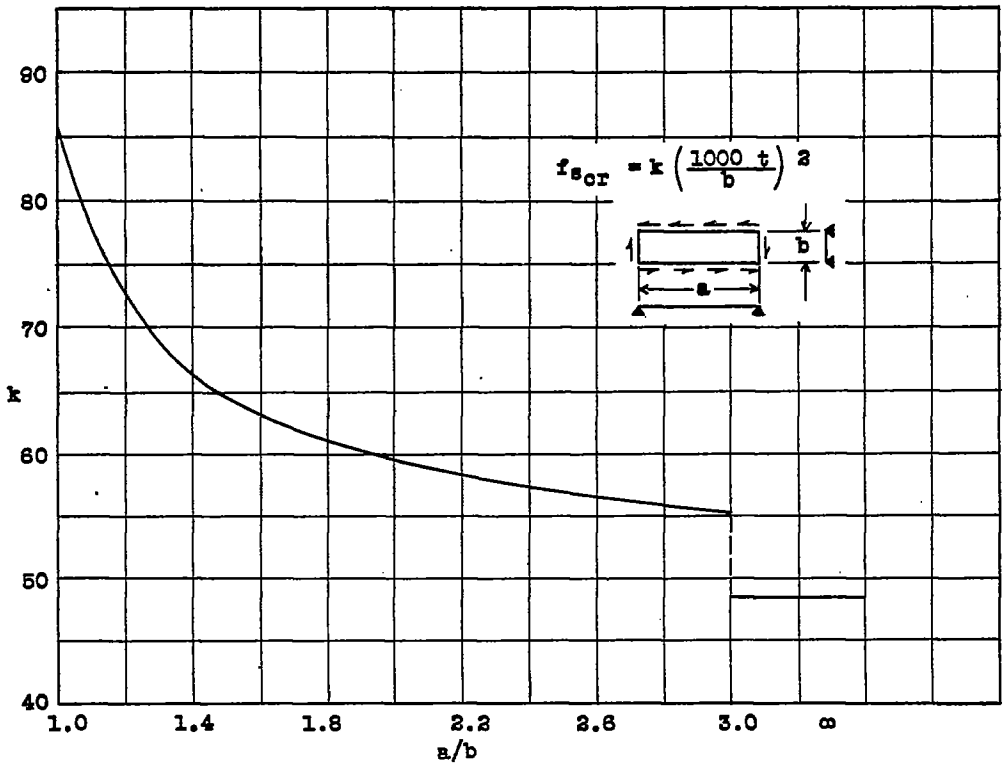

Figure 4.- Critical shearing stress for duralumin.

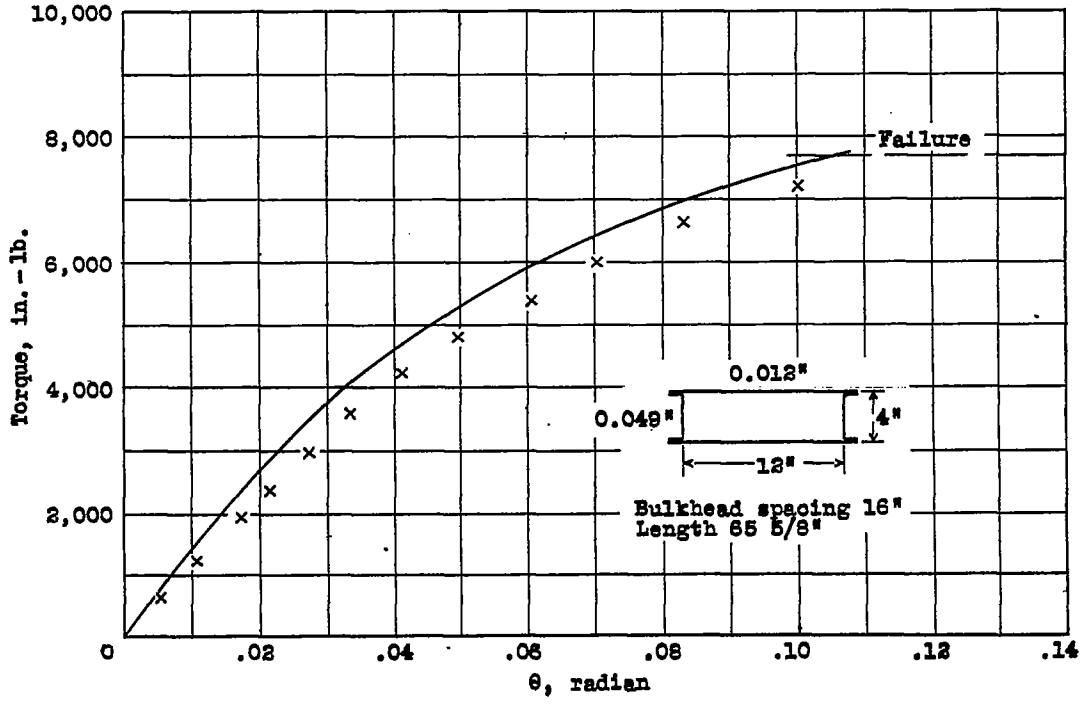

Figure 5.- Computed and experimental values of variation of angle of twist with torque for box beams. Experimental data from reference 2.

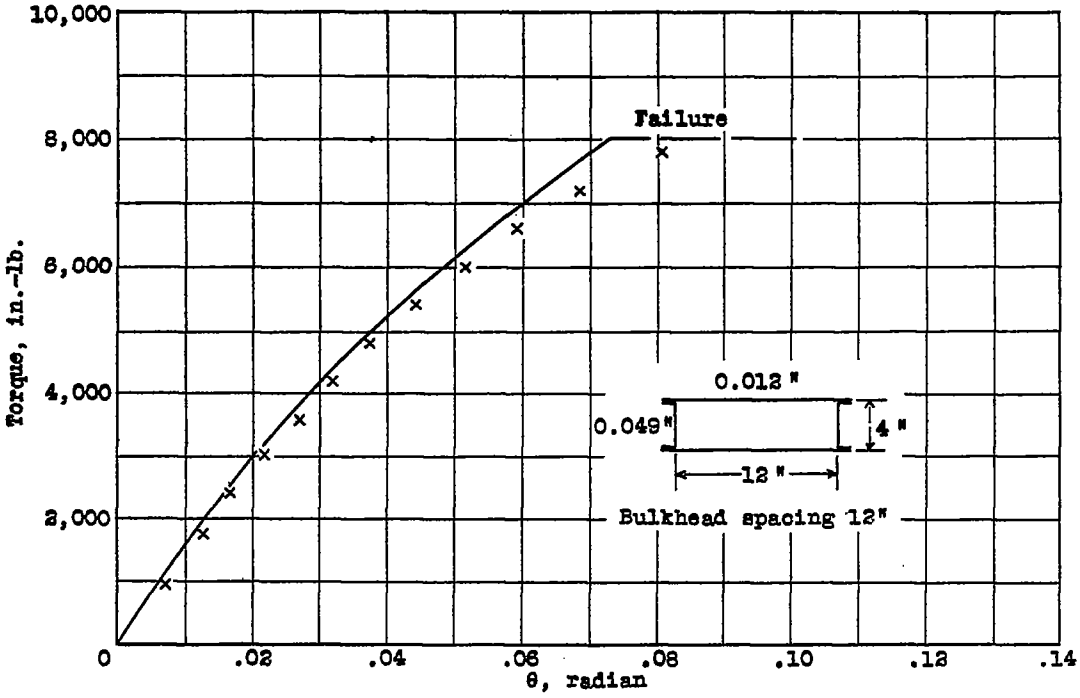

Figure 6.- Computed and experimental values of variation of angle of twist with torque for beams. Experimental data from reference 2.

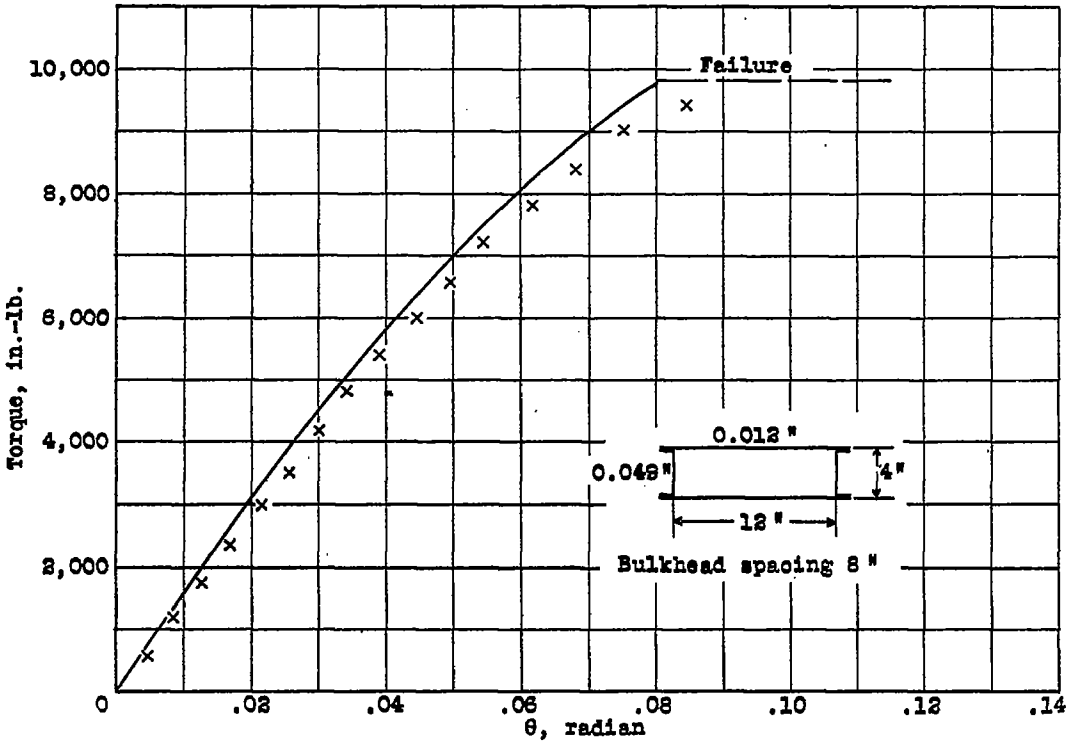

Figure 7.- Computed and experimental values of variation of angle of twist with torque for box beams. Experimental data from reference 2.

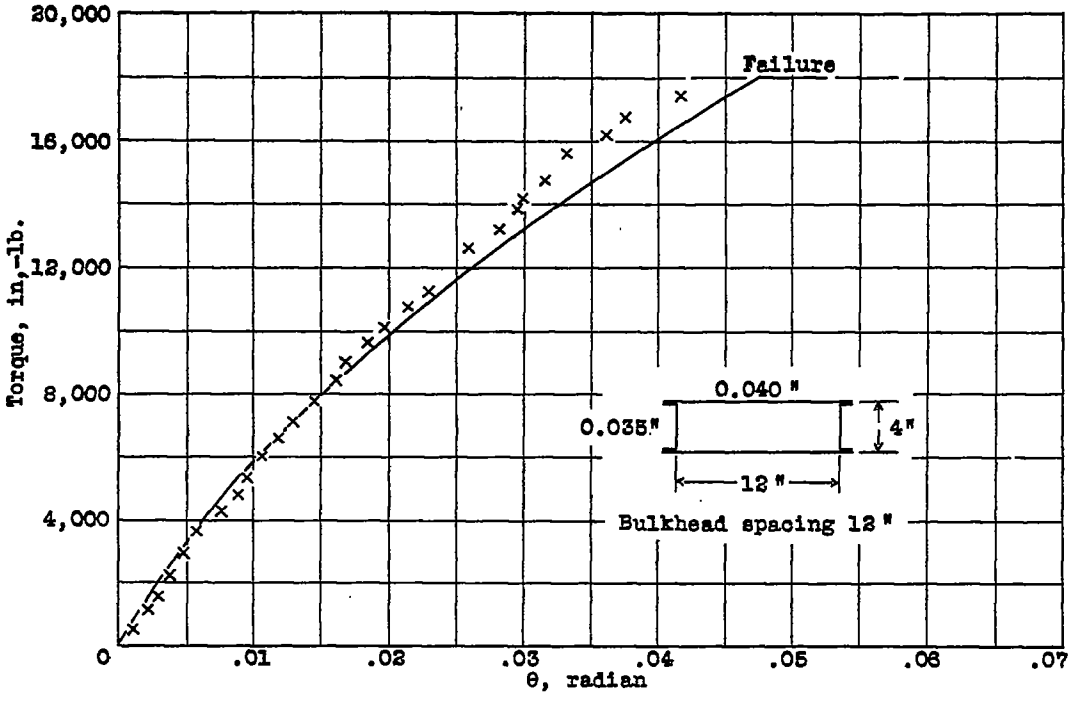

Figure 8.- Computed and experimental values of variation of angle of twist with torque for box beams. Experimental data from reference 2.

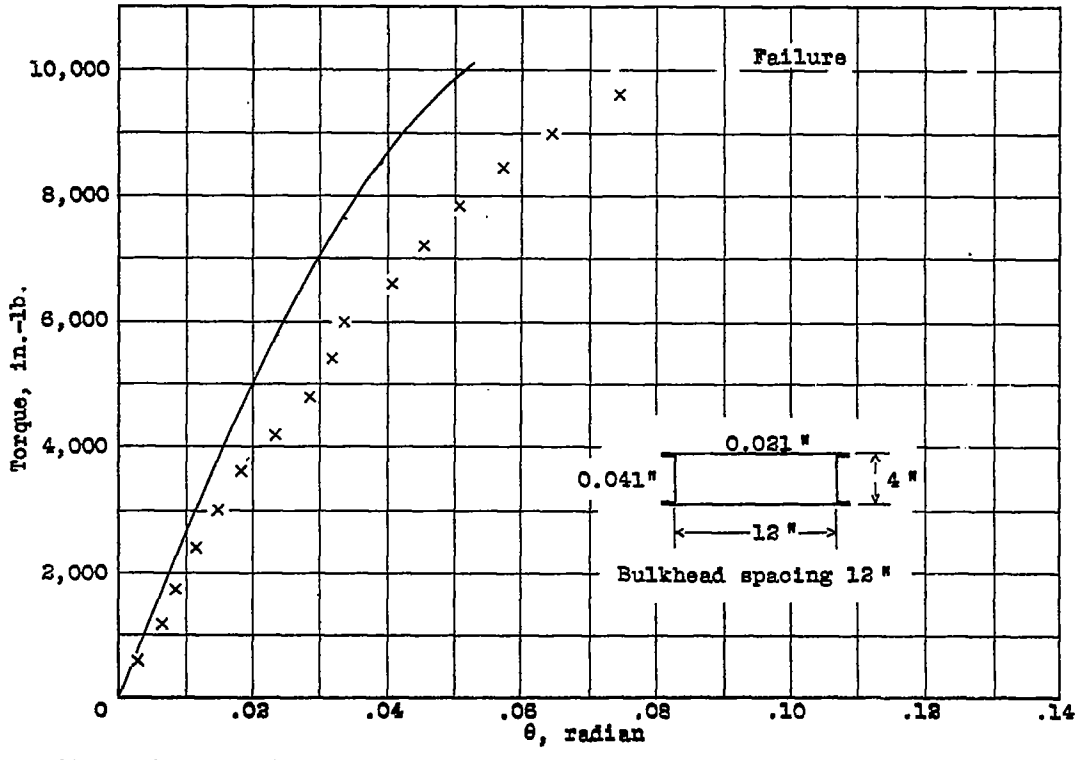

Figure 9.- Computed and experimental values of variation of angle of twist with torque for box beams. Experimental data from reference 2.

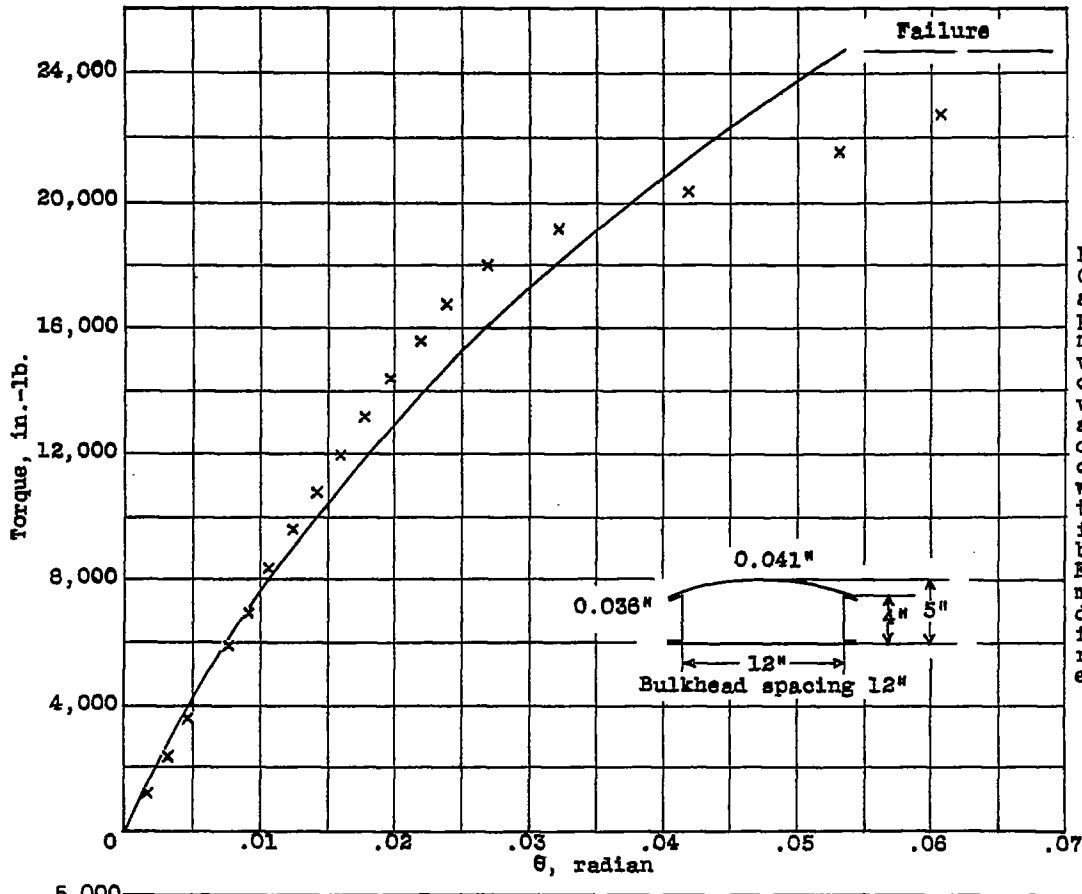

Fig.10- Computed and experimental values of variation of angle of twist with torque for box beams. Experimental data from reference 2.

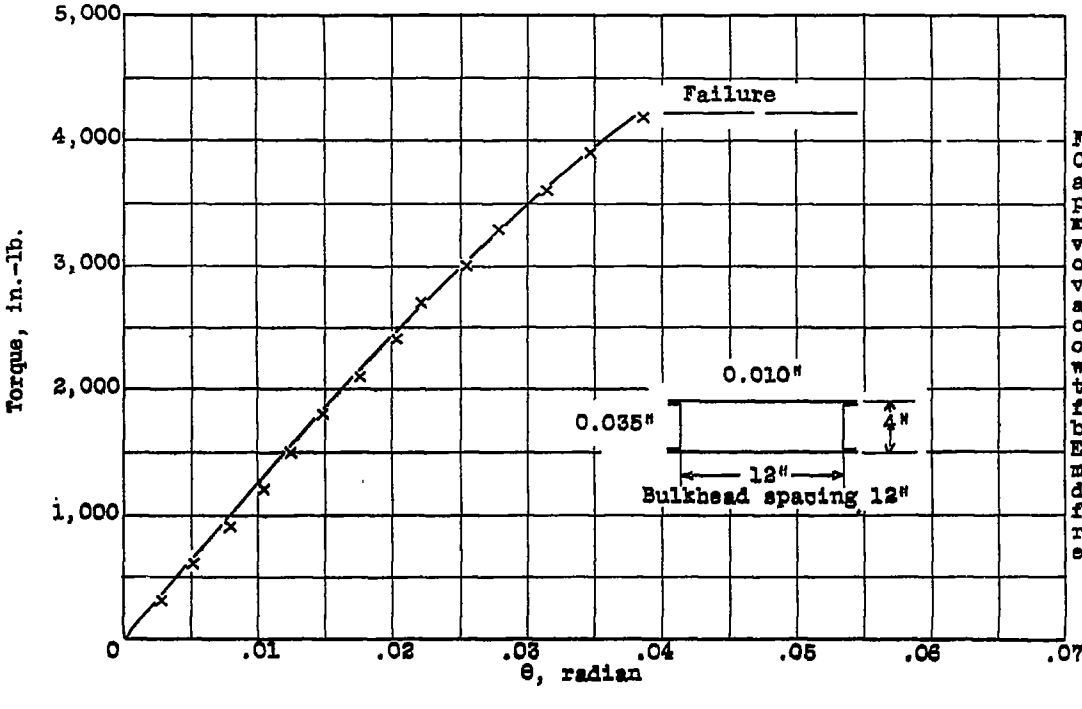

Fig.11. Computed and experimental values of variation of angle of twist with torque for box beams. Experimental data from reference 2.

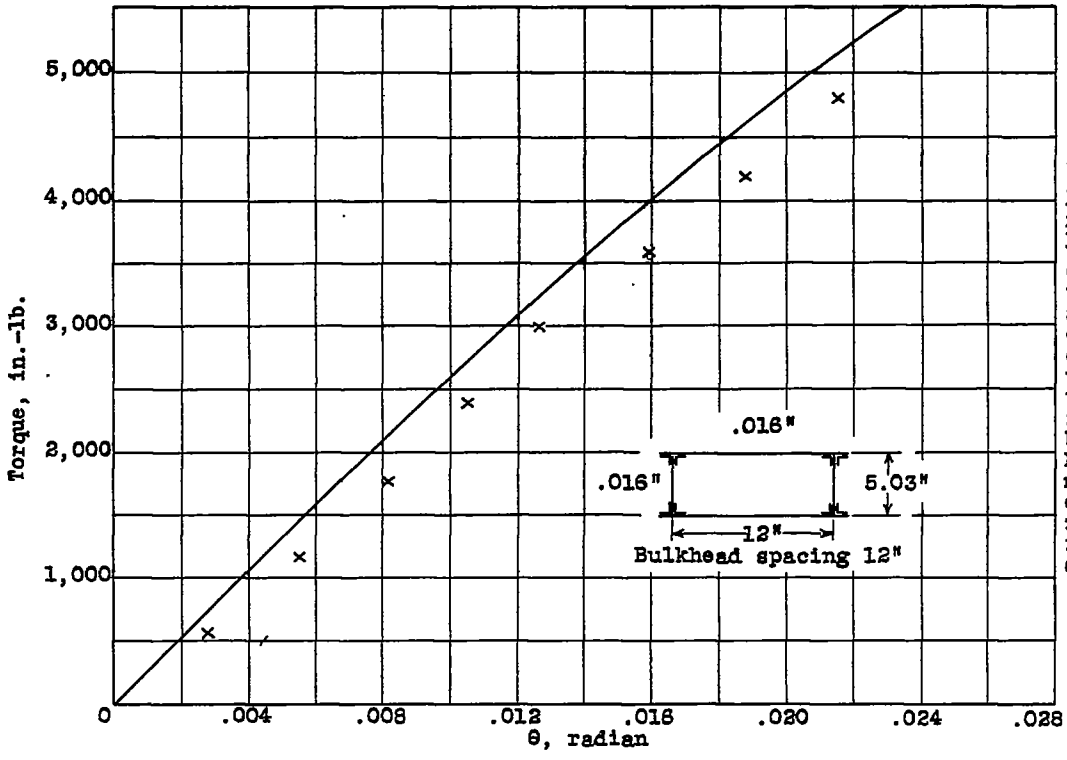

Fig.12.- Computed and experimental values of variation of angle of twist with torque for box beams. Experimental data from reference 2.

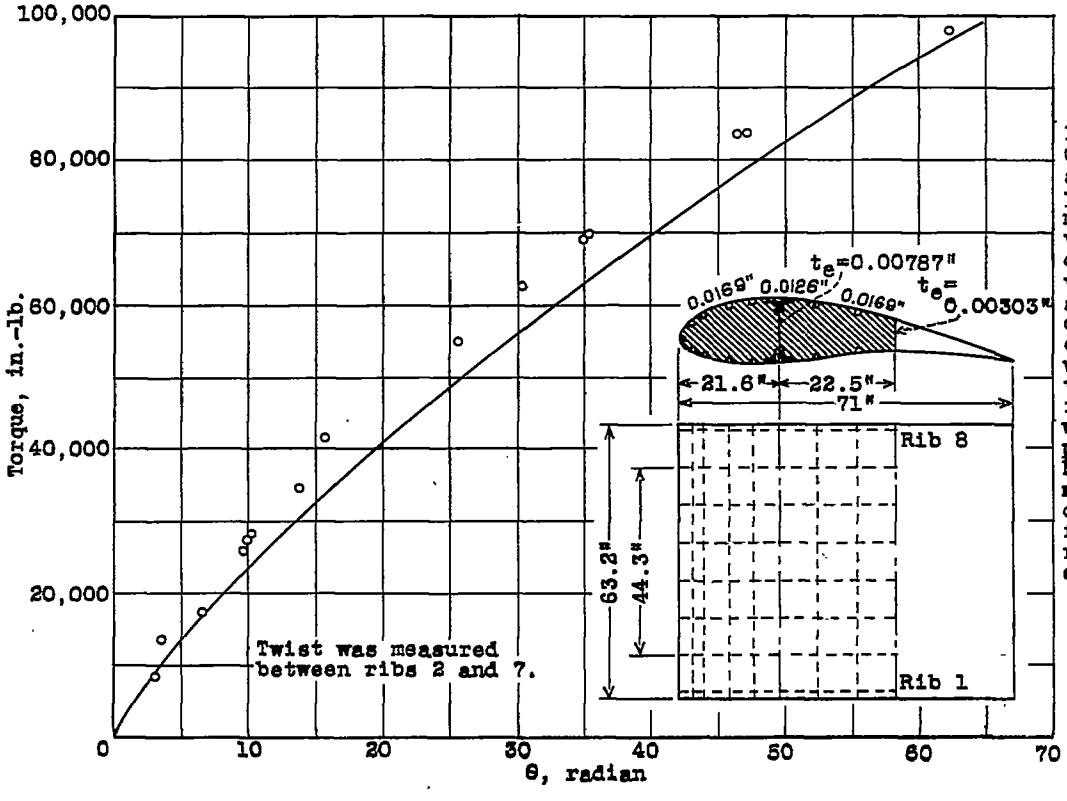

Fig.13.- Computed and experimental values of variation of angle of twist with torque for a wing panel. Experimental data from reference 5.

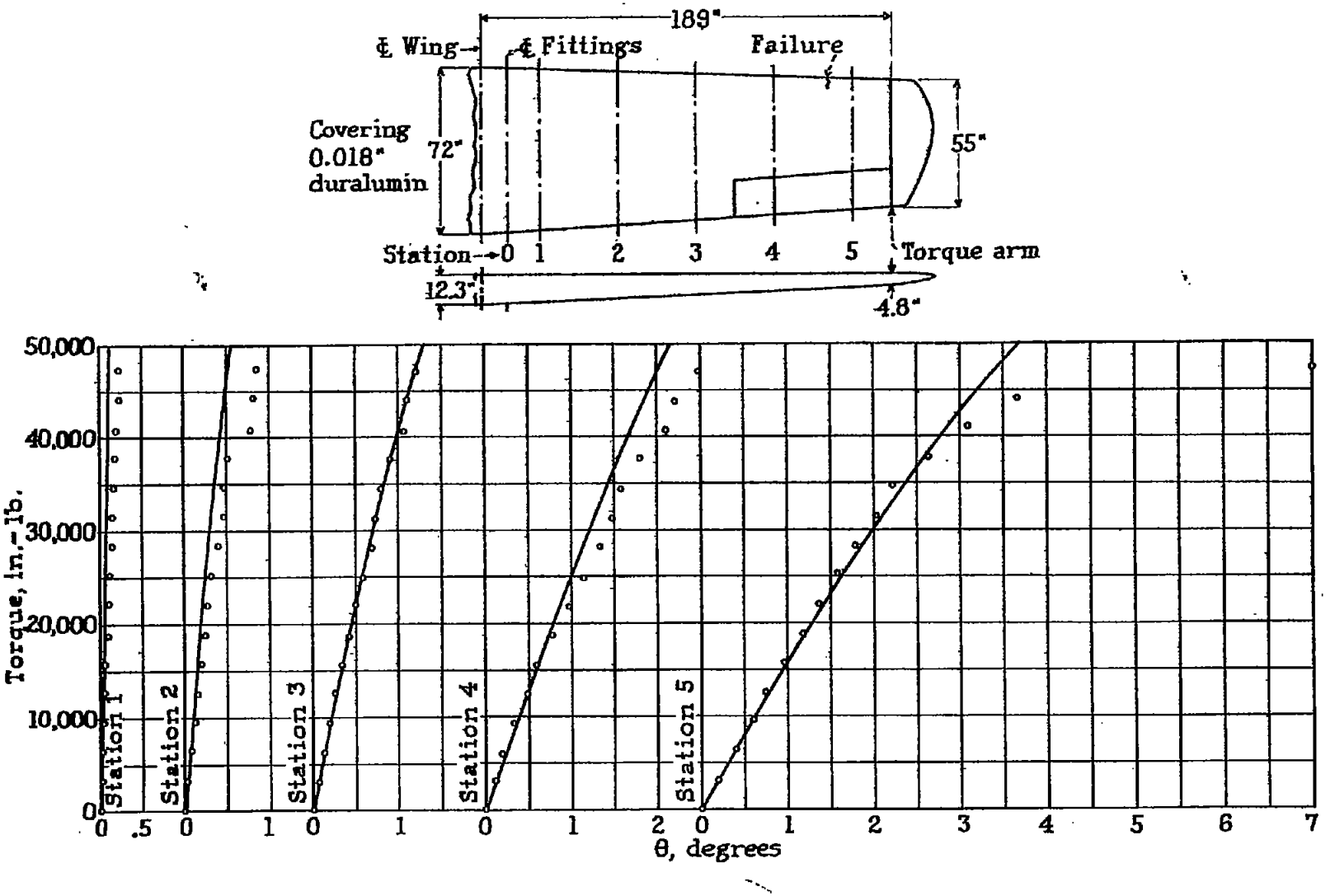

Figure 14.- Computed and experimental values of variation of angle of twist with torque for an all-metal wing. Experimental data from reference 6